SUPPORTING INFORMATION

Nearly atomic precise gold nanoclusters on nickel-based layered double hydroxides for extraordinarily efficient aerobic oxidation of alcohols

Shuai Wang, Shuangtao Yin, Gaowen Chen, Lun Li, and Hui Zhang*

State Key Laboratory of Chemical Resource Engineering, Beijing University of Chemical Technology, Beijing 100029, P. R. China.

** E-mail: huizhang67@gst21.com;*
Fax: +8610-6442 5385;
Tel: +8610-6442 5872

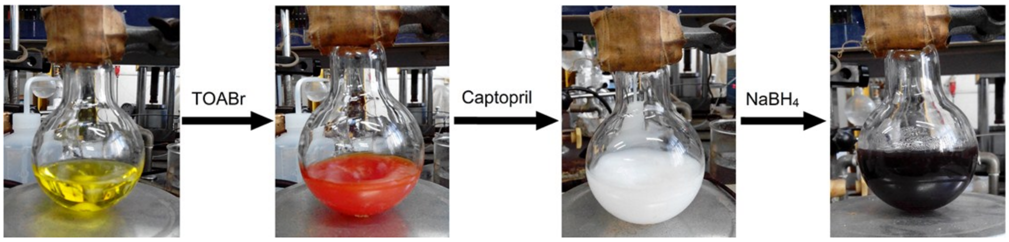

Figure S1. The color change in the preparation of $Au_{25}Capt_{18}$.

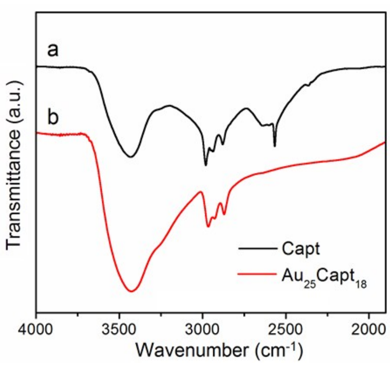

(A)

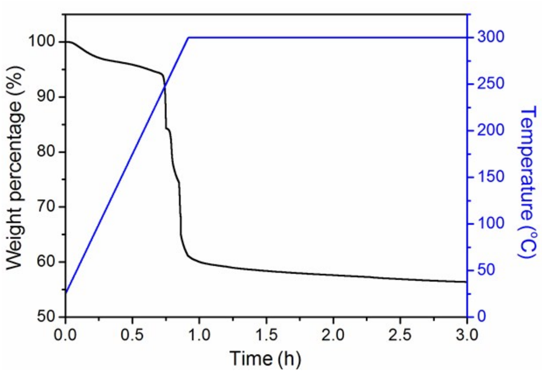

(B)

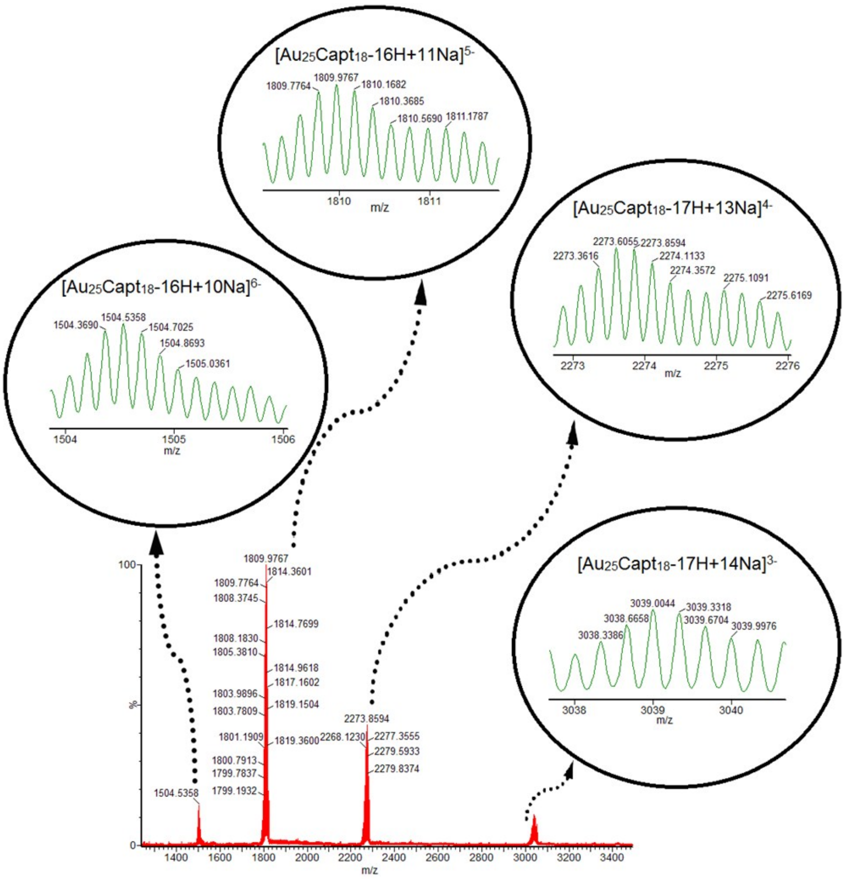

(C)

Figure S2. (A) FTIR spectra of captopril (a) and $Au_{25}Capt_{18}$ (b). (B) TG analysis of $Au_{25}Capt_{18}$. (C) Negative mode ESI-MS analysis and isotopically resolved spectra of $Au_{25}Capt_{18}$.

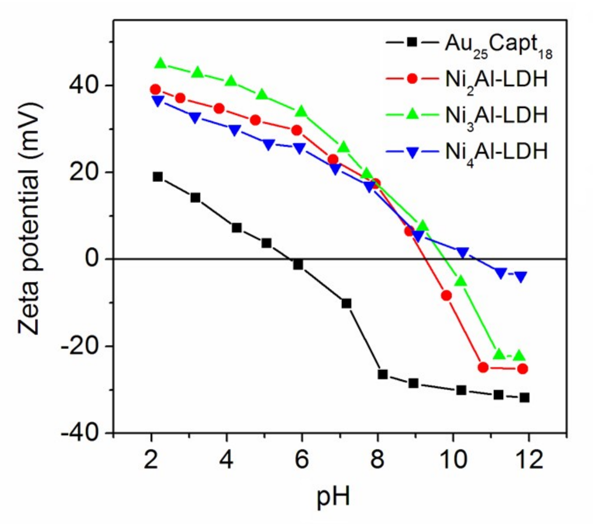

Figure S3. Variation of Zeta potential with pH image of $Au_{25}Capt_{18}$ and Ni_xAl-LDH (x = 2, 3, 4).

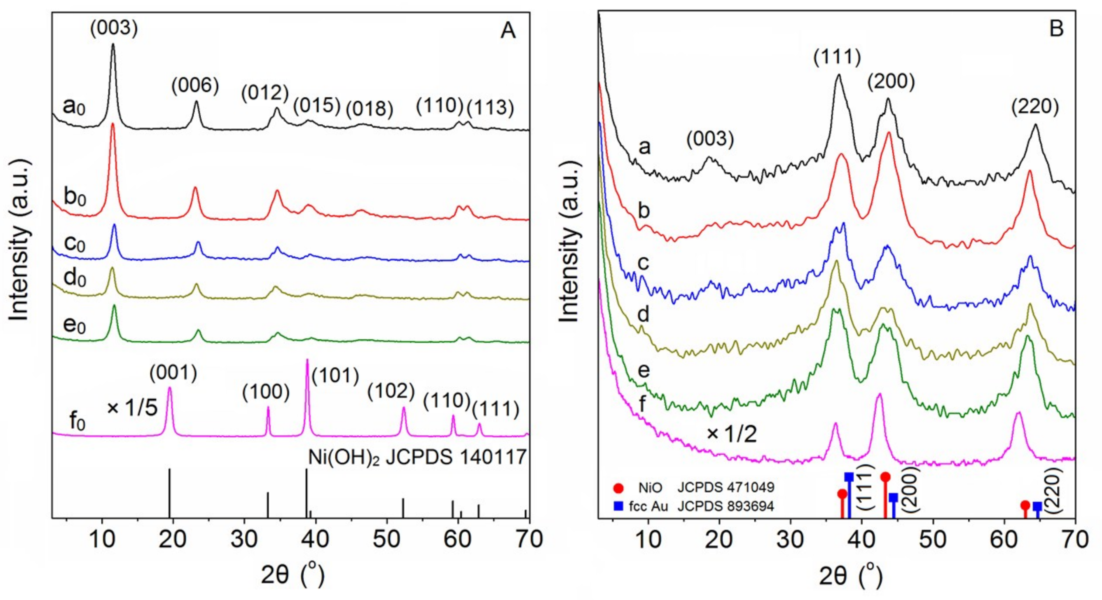

Figure S4. XRD patterns of (A) Ni_2Mn-LDH (a_0), Ni_3Mn-LDH (b_0), Ni_2MnFe-LDH (c_0), $Ni_{2.2}Mn_{0.8}Fe$-LDH (d_0), $Ni_{2.5}Mn_{0.5}Fe$-LDH (e_0), $Ni(OH)_2$ (f_0); (B) Au_{25}/Ni_2Mn-LDH (a), Au_{25}/Ni_3Mn-LDH (b), Au_{25}/Ni_2MnFe-LDH (c), $Au_{25}/Ni_{2.2}Mn_{0.8}Fe$-LDH (d), $Au_{25}/Ni_{2.5}Mn_{0.5}Fe$-LDH (e), $Au_{25}/Ni(OH)_2$ (f).

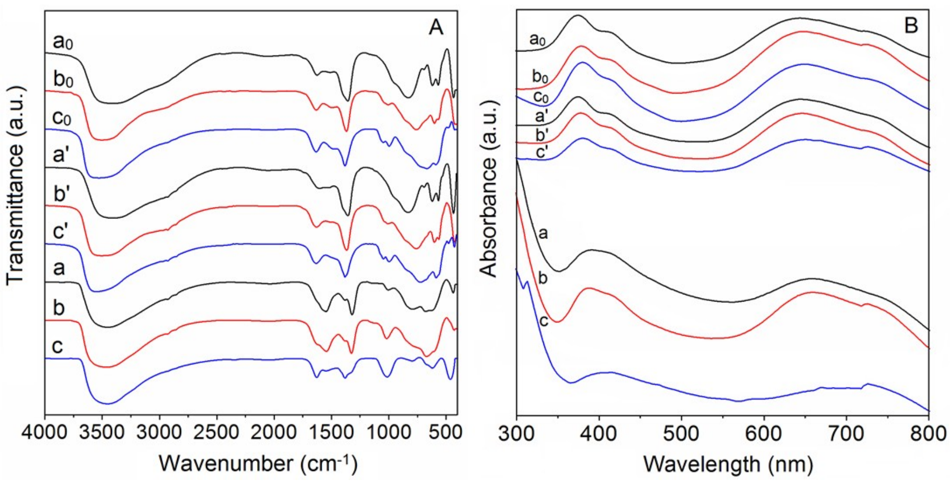

Figure S5. FTIR spectra (A) and UV-vis diffuse reflectance spectra (B) of Au_{25}/Ni_2Al-LDH (a), Au_{25}/Ni_3Al-LDH (b), Au_{25}/Ni_4Al-LDH (c), $Au_{25}Capt_{18}/Ni_2Al$-LDH (a'), $Au_{25}Capt_{18}/Ni_3Al$-LDH (b'), $Au_{25}Capt_{18}/Ni_4Al$-LDH (c'), Ni_2Al-LDH (a_0),Ni_3Al-LDH (b_0), Ni_4Al-LDH (c_0).

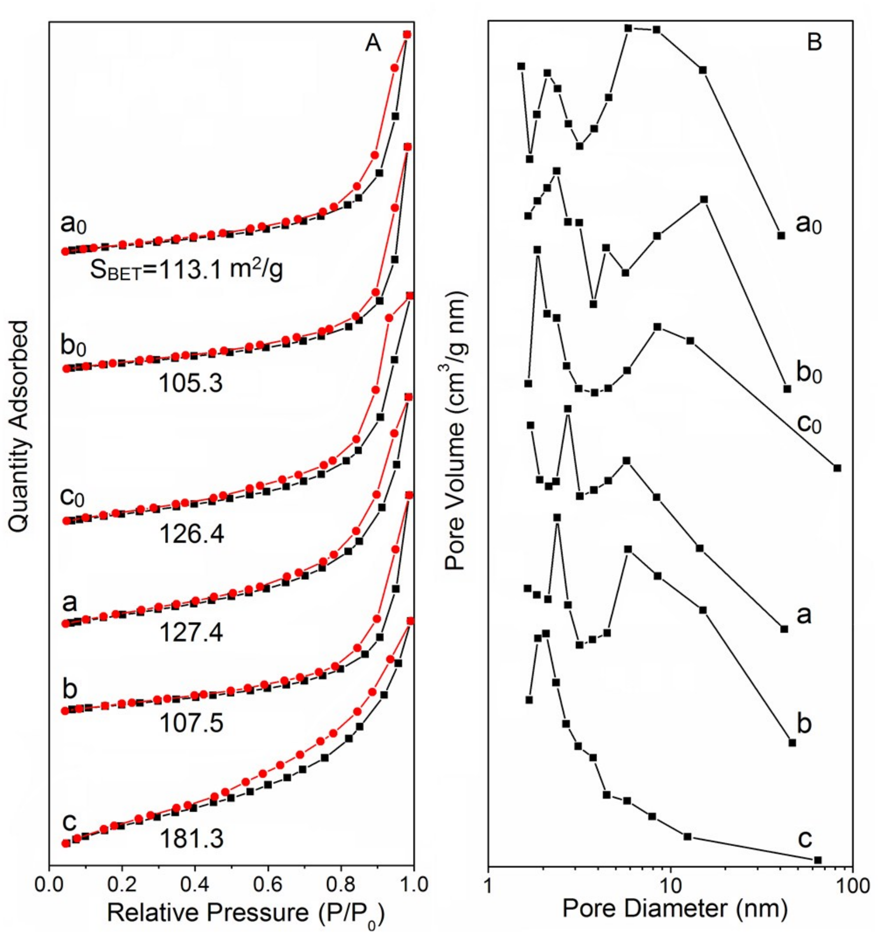

Figure S6. Nitrogen adsorption-desorption isotherms (A) and the pore size distributions (B) of Au_{25}/Ni_2Al-LDH (a), Au_{25}/Ni_3Al-LDH (b), Au_{25}/Ni_4Al-LDH (c), Ni_2Al-LDH (a_0), Ni_3Al-LDH (b_0), Ni_4Al-LDH (c_0).

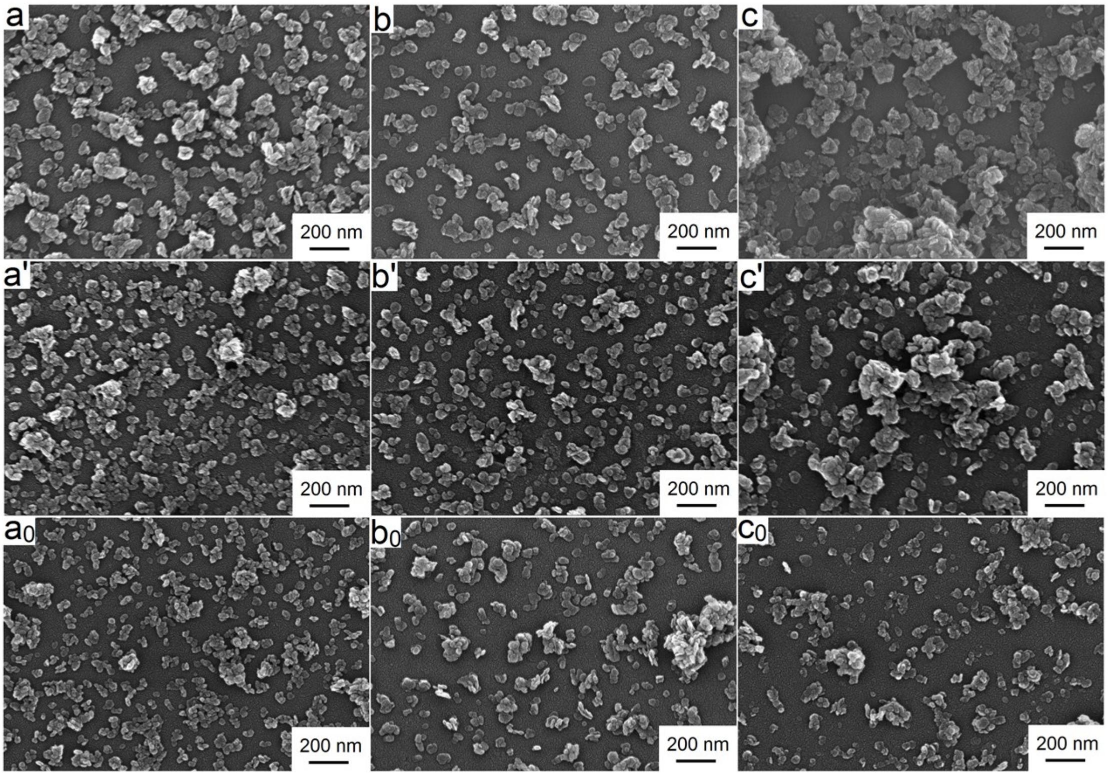

Figure S7. SEM images of Au_{25}/Ni_2Al-LDH (a), Au_{25}/Ni_3Al-LDH (b), Au_{25}/Ni_4Al-LDH (c), $Au_{25}Capt_{18}$/Ni_2Al-LDH (a'), $Au_{25}Capt_{18}$/Ni_3Al-LDH (b'), $Au_{25}Capt_{18}$/Ni_4Al-LDH (c'), Ni_2Al-LDH (a_0), Ni_3Al-LDH (b_0), Ni_4Al-LDH (c_0).

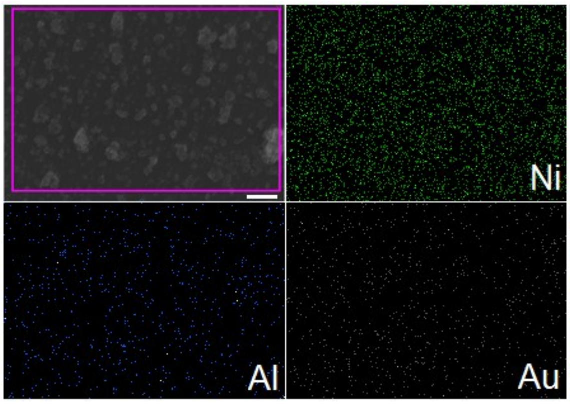

（A）

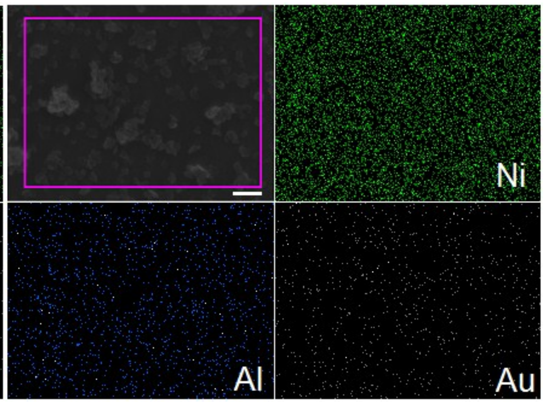

（B）

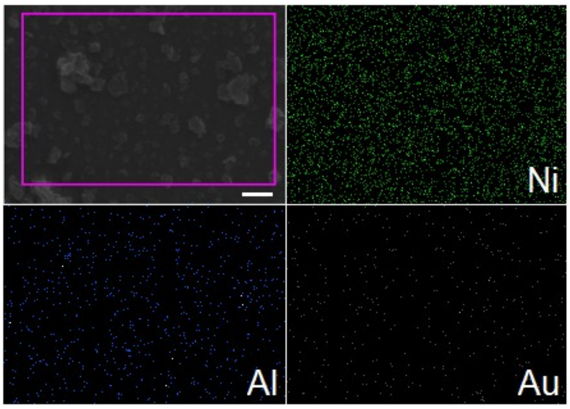

（C）

Figure S8. SEM and element mapping images of Au_{25}/Ni_2Al-LDH (A), Au_{25}/Ni_3Al-LDH (B) and Au_{25}/Ni_4Al-LDH (C). The scale bar is 200 nm.

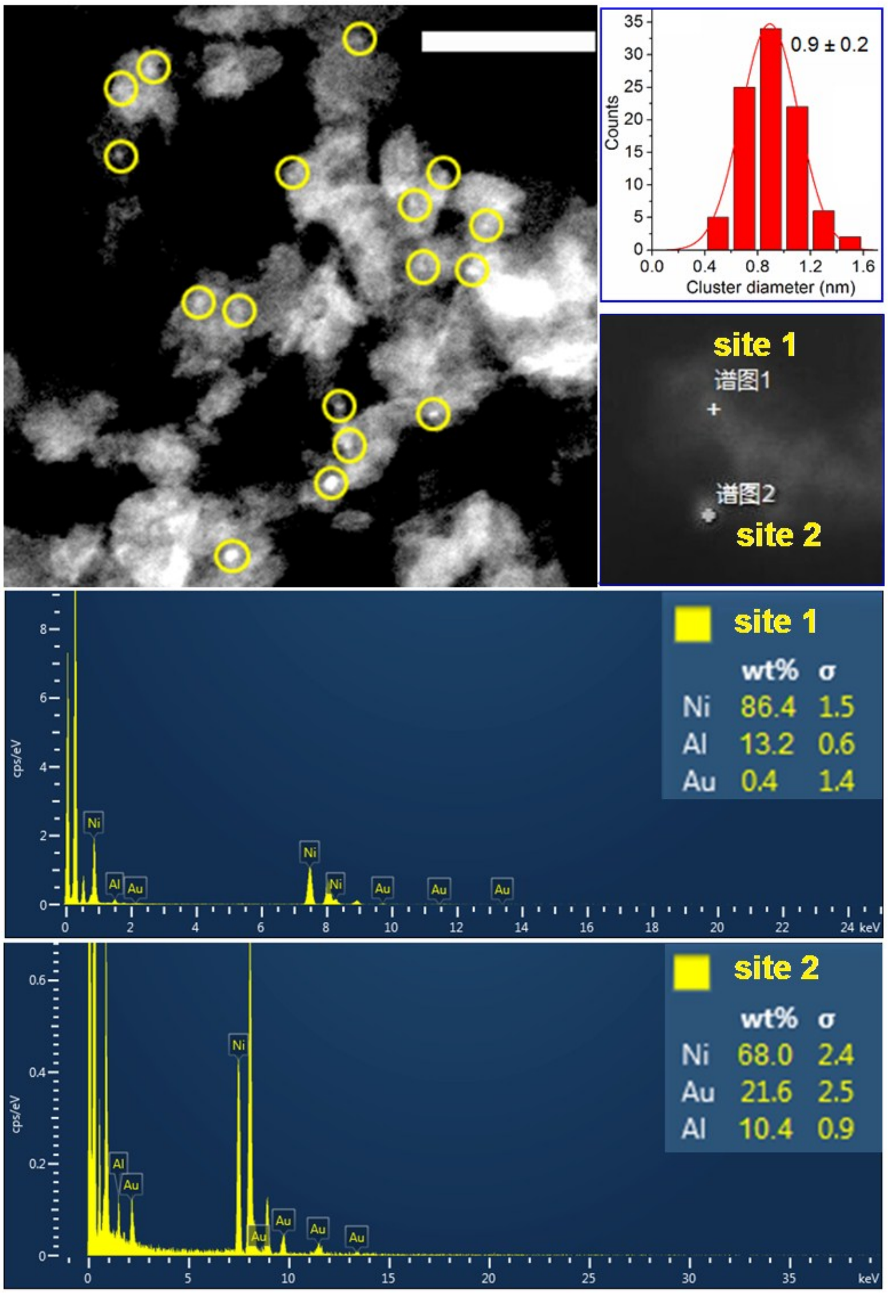

Figure S9. STEM image (scale bar: 20 nm) and Au_{25} clusters size distribution of Au_{25}/Ni_3Al-LDH and EDX spectra at different sites in STEM.

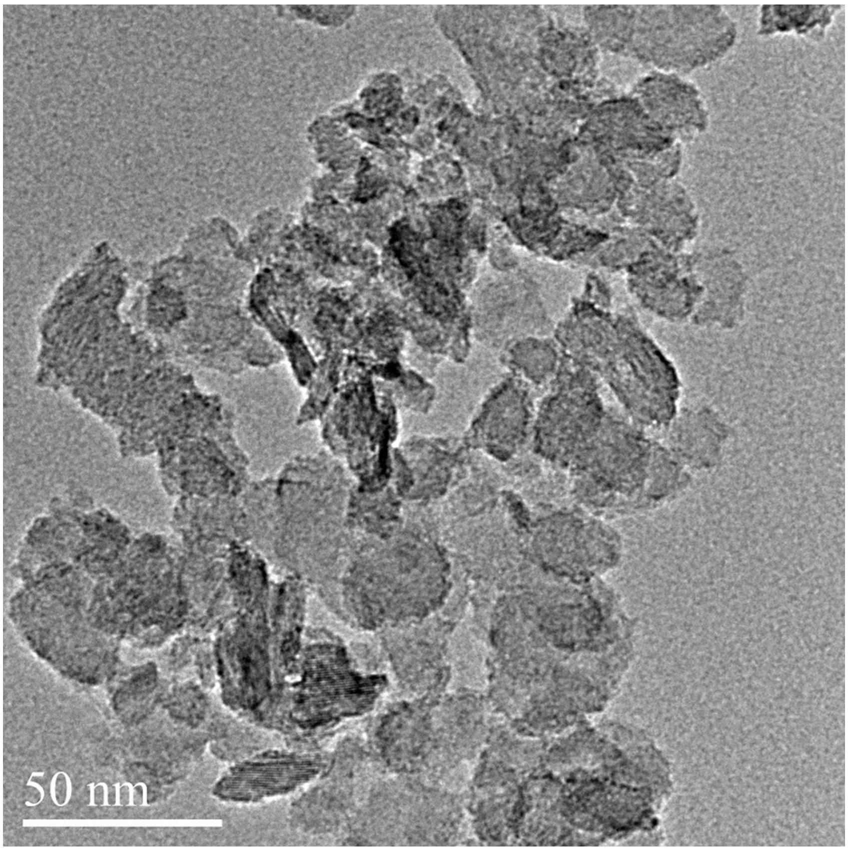

Figure S10. HRTEM image of the recovered catalyst of Au_{25}/Ni_3Al-LDH after five runs.

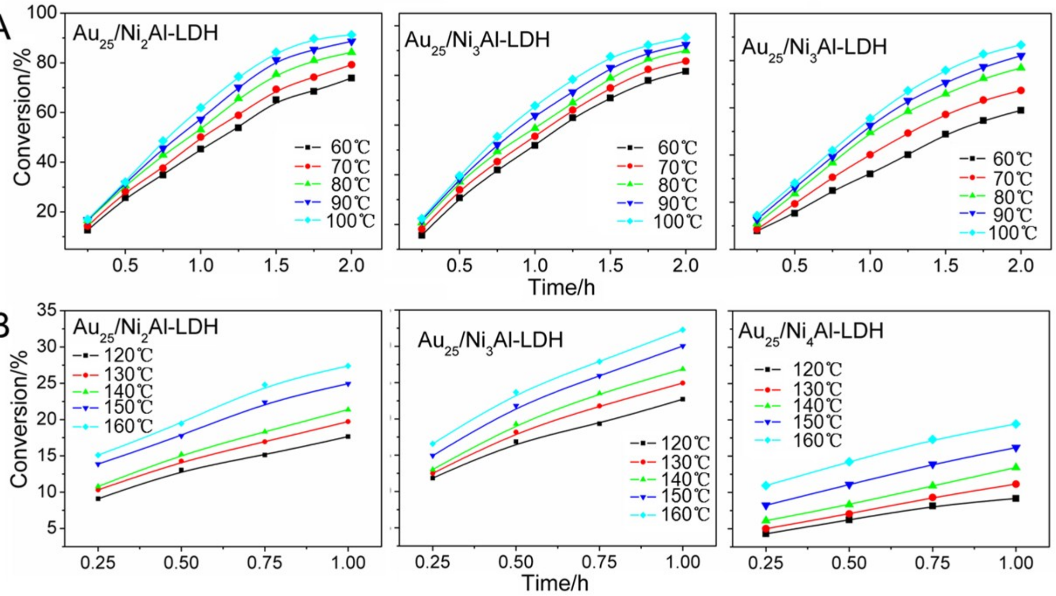

Figure S11. Time-conversion plots for the aerobic oxidation of 1-phenylethanol over Au_{25}/Ni_xAl-LDH catalysts at varied temperatures in toluene (A) and solvent-free (B).

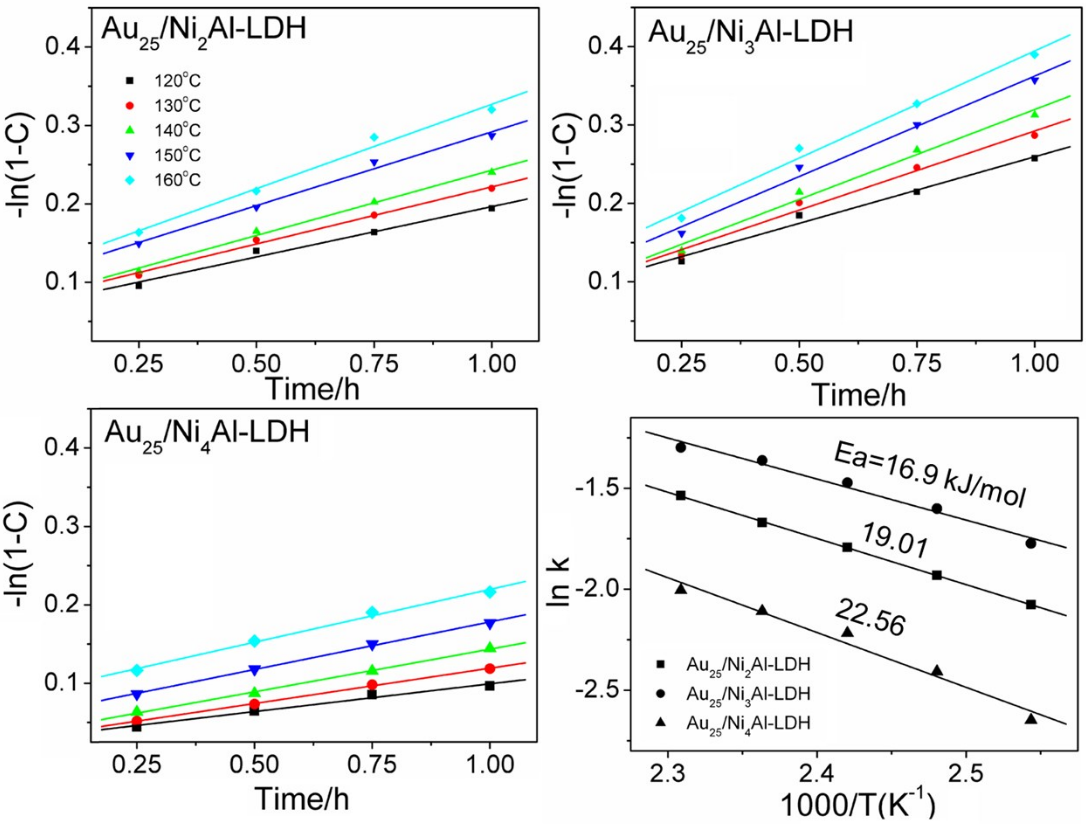

Figure S12. -ln(1-*C*) against time and Arrhenius plots for the aerobic oxidation of 1-phenylethanol catalyzed by Au_{25}/Ni_xAl-LDH (x = 2, 3, 4) at temperatures between 120 and 160 ^{o}C. Reaction conditions: 1-phenylethanol (100 mmol), catalyst (Au: 4.0×10^{-4} mol%), O_2 (20 mL/min).

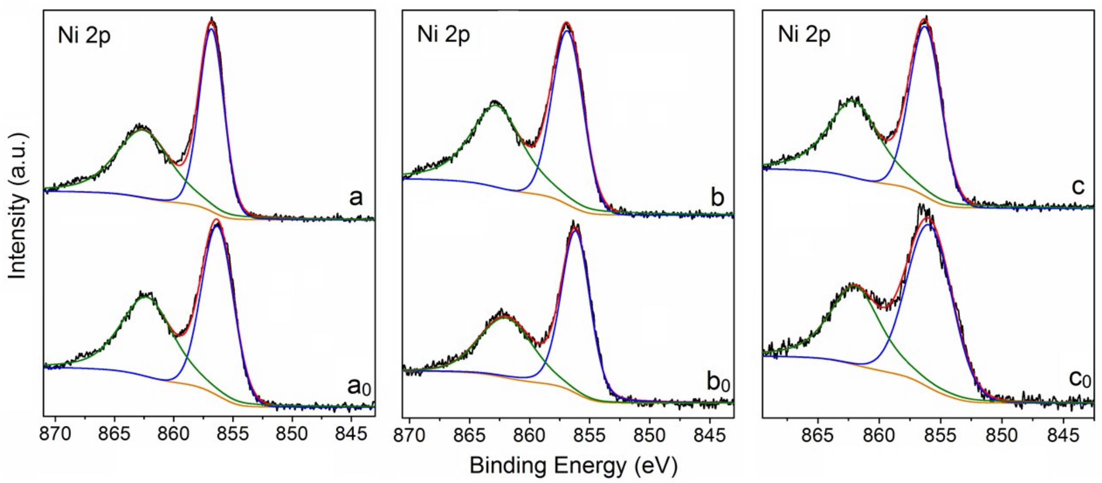

Figure S13. Ni 2p XPS spectra of Au_{25}/Ni_2Al-LDH (a), Au_{25}/Ni_3Al-LDH (b), Au_{25}/Ni_4Al-LDH (c), Ni_2Al-LDH (a_0), Ni_3Al-LDH (b_0), Ni_4Al-LDH (c_0).

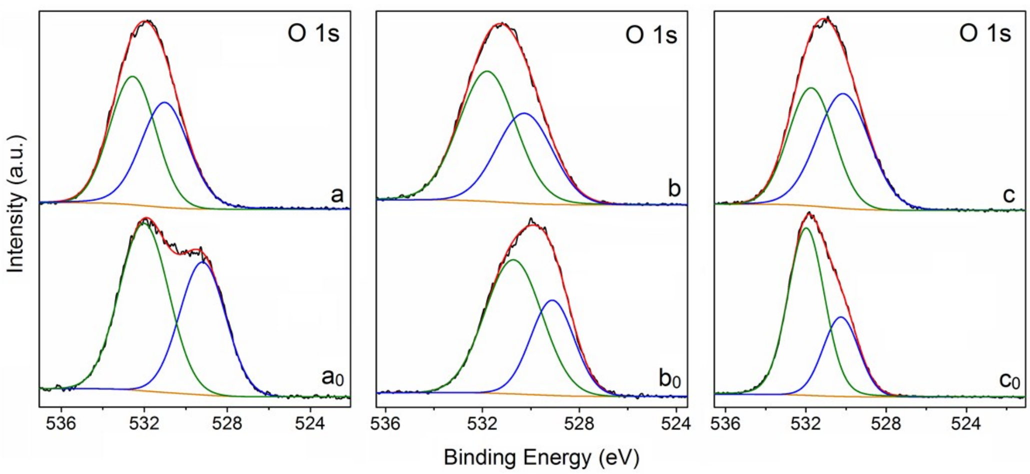

Figure S14. O 1s XPS spectra of Au_{25}/Ni_2Al-LDH (a), Au_{25}/Ni_3Al-LDH (b), Au_{25}/Ni_4Al-LDH (c), Ni_2Al-LDH (a_0), Ni_3Al-LDH (b_0), Ni_4Al-LDH (c_0).

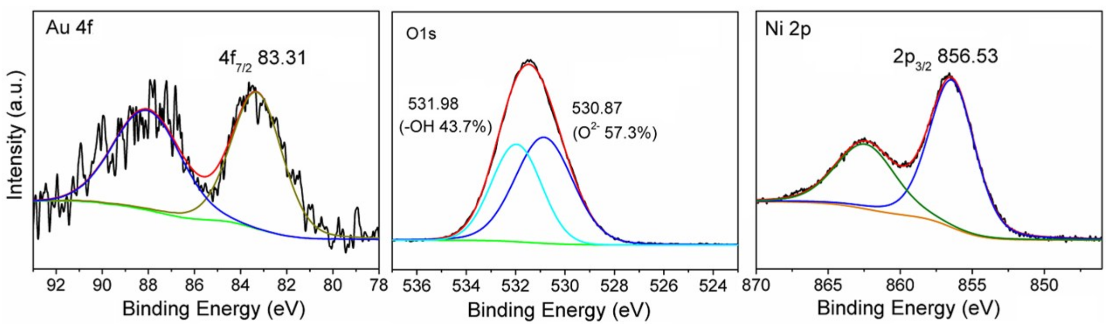

Figure S15. Au 4f, O 1s and Ni 2p XPS spectra of the recovered Au_{25}/Ni_3Al-LDH catalyst.

Table S1. XRD parameters of Ni_xAl-LDH (x = 2, 3, 4), $Au_{25}Capt_{18}/Ni_xAl$-LDH and Au_{25}/Ni_xAl-LDH.

Samples	d_{003} (nm)	d_{110} (nm)	c (nm)[a]	a (nm)[a]	D_{003} (nm)[b]	D_{110} (nm)[b]	Ni^{2+}/Al^{3+} [c]	x[d]	S (nm^2/charge)[e]
Ni_2Al-LDH	0.745	0.1509	2.235	0.3018	14.442	18.273	1.96	0.34	0.23
Ni_3Al-LDH	0.760	0.1516	2.280	0.3032	13.767	23.794	3.02	0.25	0.32
Ni_4Al-LDH	0.766	0.1520	2.298	0.3040	11.785	15.711	3.88	0.20	0.40
$Au_{25}Capt_{18}/Ni_2Al$-LDH	0.747	0.1508	2.241	0.3016	13.091	16.316	1.96	0.34	--
$Au_{25}Capt_{18}/Ni_3Al$-LDH	0.762	0.1517	2.286	0.3034	14.018	19.826	3.02	0.25	--
$Au_{25}Capt_{18}/Ni_4Al$-LDH	0.772	0.1522	2.316	0.3044	11.784	18.589	3.88	0.20	--
Au_{25}/ Ni_2Al-LDH	0.659	0.1504	1.977	0.3008	9.198	15.502	1.96	0.34	--
Au_{25}/ Ni_3Al-LDH	0.663	0.1512	1.989	0.3024	8.154	7.870	3.02	0.25	--
Au_{25}/ Ni_4Al-LDH	--	--	--	--	--	--	3.88	0.20	--

[a]Based on hexagonal crystal system, $a = 2d_{110}$, $c = 3d_{003}$. [b]Estimated by Scherrer equation $D_{(hkl)} = 0.89\lambda/\beta\cos\theta$. [c]Determined by ICP-AES. [d]Calculated upon ICP data: x = Al/(Ni + Al). [e]S: available surface area per unit charge of the LDH layer. $S_{unit\text{-}charge} = (a^2 \sin 60)/x$.

Table S2. Rate constants for aerobic oxidation of 1-phenylethanol by Au_{25}/Ni_xAl-LDH (x = 2, 3, 4) catalysts in toluene.[a]

Catalysts	k (h^{-1})				
	60 °C	70 °C	80 °C	90 °C	100 °C
Au_{25}/Ni_2Al-LDH	0.7036	0.827	0.9997	1.2005	1.3895
	(0.9933)[b]	(0.9944)	(0.9909)	(0.9877)	(0.9858)
Au_{25}/Ni_3Al-LDH	0.8915	1.0219	1.1986	1.3557	1.6256
	(0.9951)	(0.9902)	(0.9803)	(0.9853)	(0.9838)
Au_{25}/Ni_4Al-LDH	0.4789	0.6081	0.7911	0.9257	1.1018
	(0.9956)	(0.9984)	(0.9988)	(0.9969)	(0.9923)

[a]Reaction conditions: 1-phenylethanol (5 mmol), catalyst (Au: 0.01 mol%), toluene (5 mL), O_2 (20 mL/min).
[b]The figures in parentheses represent R^2.

Table S3. Rate constants for aerobic oxidation of 1-phenylethanol by Au_{25}/Ni_xAl-LDH (x = 2, 3, 4) catalysts in solvent-free.[a]

Catalysts	k (h^{-1})				
	120 °C	130 °C	140 °C	150 °C	160 °C
Au_{25}/Ni_2Al-LDH	0.1283	0.1457	0.1664	0.1882	0.2152
	(0.9832)[b]	(0.9935)	(0.9942)	(0.9908)	(0.9865)
Au_{25}/Ni_3Al-LDH	0.1698	0.2017	0.2293	0.2261	0.2730
	(0.9838)	(0.9856)	(0.9858)	(0.9884)	(0.9895)
Au_{25}/Ni_4Al-LDH	0.0708	0.09	0.1089	0.1214	0.1347
	(0.9839)	(0.9989)	(0.9979)	(0.9985)	(0.9935)

[a]Reaction conditions: 1-phenylethanol (100 mmol), catalyst (Au: 4.0 × 10^{-4} mol%), O_2 (20 mL/min). [b]The figures in parentheses represent R^2.

Table S4. XPS analysis of Au_{25}/Ni_xAl-LDH catalysts compared with Ni_xAl-LDH supports.

Samples	Au $4f_{7/2}$ (eV)	Δ BE (eV)[a]	Ni $2p_{3/2}$ (eV)	O 1s (eV) (-OH)	O 1s (eV) (O^{2-})
Au_{25}/Ni_2Al-LDH	83.42	0.58	856.80	532.56 (52.40%)	531.01 (47.60%)
Ni_2Al-LDH	--	--	856.27	532.01 (57.39%)	529.19 (42.61%)
Au_{25}/Ni_3Al-LDH	83.34	0.66	856.84	531.80 (60.52%)	530.26 (39.48%)
Ni_3Al-LDH	--	--	856.16	531.22 (64.68%)	529.61 (35.32%)
Au_{25}/Ni_4Al-LDH	83.52	0.48	856.25	531.73 (46.56%)	530.13 (53.44%)
Ni_4Al-LDH	--	--	855.90	531.98 (69.33%)	530.25 (30.67%)

[a]Relative binding Energy of Au $4f_{7/2}$ of Au_{25}/Ni_xAl-LDH compared with the bulk Au (84.0 eV).